International Journal of Steel Structures
June 2010, Vol 10, No 2, 177-191

International Journal of
STEEL
STRUCTURES
www.ijoss.org

Seismic Design, Performance, and Behavior of Composite-Moment Frames with Steel Beam-to-Concrete Filled Tube Column Connections

Jong-Wan Hu[1], Yoon-Sig Kang[2], Dong-Ho Choi[3], and Taehyo Park[3,*]

[1]*Research Assistant Professor, Department of Civil and Environmental Engineering, Hanyang University, Seoul, 133-791, Korea*
[2]*Doctorate Candidate, Department of Civil and Environmental Engineering, Hanyang University, Seoul, 133-791, Korea*
[3]*Professor, Department of Civil and Environmental Engineering, Hanyang University, Seoul, 133-791, Korea*

Abstract

Concrete filled steel tube (CFT) columns have been widely used in composite-moment frames (C-MFs) both in non-seismic and in high seismic zones. The objective of this research is to develop a design methodology of such moment resisting frame structures designed with CFT columns in achieving ductile behavior and high strength. These composite-moment frames mostly constructed around the perimeter of the building provide the enough stiffness to withstand the lateral displacement due to wind or seismic loads. In this research, three sets of prototype composite frame models were designed on the basis of the proposed design examples as 3-, 9-, and 20-story post-Northridge SAC buildings with composite-special moment frame (C-SMF) systems designed for the western US area. The exact moment-rotational behavior of steel beam-to-CFT column connections including the strength degradation was simulated using the 2D joint model with the rigid boundary element. Nonlinear pushover analyses were conducted on the numerical frame models so as to evaluate the over-strength, inelastic deformation, and P-Delta effect for the entire structure. The statistical investigation was introduced to nonlinear dynamic analyses under 40 SAC ground motions corresponding to a seismic hazard level of 2% probability of exceedence in 50 years in order to efficiently examine seismic performance and behavior of entire composite frame structures. All frame models meet the allowable limit for safe designs. In addition, the entire frame design becomes conservative as the number of stories increases. The distribution of inter-story drift ratios (ISDRs) as well as the over-strength ratio also demonstrates this conservative design of low to high-rise C-MF structures.

Keywords: composite-moment frame, concrete-filled tube column, 2D joint model, nonlinear frame analyses, inter-story drift ratio

1. Introduction

In the latest years, concrete filled steel tube (CFT) structures have become accepted and used in multistory buildings as well as bridge piers on the ground that they can provide the enhanced advantages of ductility associated with steel structures and high compressive strength associated with inside concrete components (Roeder, 2000). The advantages of CFT columns over other steel-concrete composite structures called either mixed or hybrid systems include the fact that inside concrete prevents local buckling of steel tube wall and that the steel tube extends the ability of concrete spalling (Azizinamini and Schneider, 2001; Hajjar, 2002; Kim *et al*., 2008). In words, the advantages of two materials can be utilized while their disadvantages can be compensated. The reduced usage of steel would result in improved fire resistance and significant cost reduction in comparison with traditional steel construction. The steel tubes can be accepted as the mold and supporting structures for casting concrete in construction. Therefore, CFT structures have improved constructability rather than conventional reinforced concrete structures (Morino *et al*., 2001).

Composite CFT columns are especially suited for moment resisting frames as the most common lateral-force resisting structures in the high seismic areas because they have a high strength to weight ratio due to the confinement effect of concrete core, provide excellent monotonic and dynamic resistance under biaxial bending plus axial force, and improve damping behavior (Tsai *et al*., 2004). Composite special moment frames (C-SMFs) consisting of steel I girders and either rectangular or

Note.-Discussion open until November 1, 2010. This manuscript for this paper was submitted for review and possible publication on October 20, 2009; approved on May 11, 2010.

*Corresponding author
Tel: +82-2-2220-0321; Fax: +82-2-2220-4322
E-mail: cepark@hanyang.ac.kr

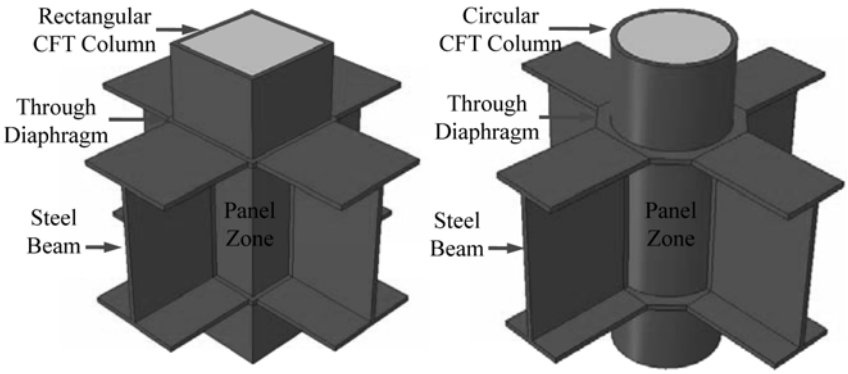

Figure 1. Typical steel beam-to-concrete filled tube column connections.

circular CFT columns (RCFT or CCFT columns) are mostly located on the perimeter of the building because they are economical and efficient force resisting systems (SFRSs) as recognized in Section 9/Part II of the current 2005 AISC Seismic Provisions (ANSI/AISC 341-05, 2005). In these systems, deformations due to seismic actions are accommodated by the formation of hinges in the beams and stability is assured through the enforcement of strong column-weak beam mechanisms in design (Tsai *et al*., 2008). Typical connection configurations installed on these C-MFs include fully restrained (FR) steel beam-to-concrete filled tube (CFT) column connections as illustrated in Fig. 1.

This paper discusses the design of such frames in accordance with the advanced criteria introduced in the 2005 AISC Seismic Provisions (ANSI/AISC 341-05) and the ASCE 7-05 guidelines (ASCE, 2005). The 2005 Seismic Provisions explicitly allow the use of the full plastic capacities of CFT columns even for columns with more slender steel walls than ones allowed in previous design specifications. Load combinations (LCs) including gravity and lateral loads were determined following the ASCE 7-05 guidelines (ASCE, 2005) and the IBC 2006 (IBC, 2006). Design limits, system requirements, and seismicity factors for these buildings located on a high seismicity area were also specified in these guidelines. However, most of currently established researches have only concentrated on the local members such as composite panel zones and CFT columns rather than whole C-MF structures. Due to the motivation to compensate for lack of related researches, this study will focus particularly on the seismic design and performance of entire composite-moment resisting frames accompanied with both linear and nonlinear analyses utilizing equivalent static-lateral and dynamic loads. The static and seismic behavior of C-MFs was simulated by the numerical frame models with simplified 2D joint models, meaning that the exact moment-rotation behavior of composite panel zones was taken into consideration during numerical simulations. These numerical models were implemented in the Open System for Earthquake Engineering Simulation (Open SEES) (Mazzoni *et al*., 2006), an open source program widely used in the USA for this type of study and calibrated to test data. The results of numerical simulations were used to validate the adequacy of the design based on the performance of the overall moment frame in terms of inter-story drift ratios (ISDRs).

2. Overview of Current US Design Specification

The design provisions based on the full plastic behavior of composite members and systems are particularly important in limit state calculations for non-seismic and seismic resistant design. The current code provisions for composite construction - namely, American Institute of Steel Construction 2005 Specification (ANSI/AISC No. 360-05) and Seismic Provisions (ANSI/AISC 341-05) - are increasingly presenting engineers with new guidance on the analysis and design of composite columns and moment frames. The current AISC code provisions for composite columns are appropriate to predict the ultimate capacity of CFT beam-columns corresponding to the full plastic stress distribution of a cross section area according to the variable position of the neutral axis under eccentric loading. Concrete is a brittle material with considerably different response in between tension and compression. Design codes generally neglect tensile stiffness at concrete materials. AISC 2005 Seismic Provisions address four types of composite moment resisting frames: (a) composite-partially restrained moment frames (C-PRMF), (b) composite-special moment frames (C-SMF), (c) composite-intermediate moment frames(C-IMF), and (d) composite-ordinary moment frames (C-OMF). The development of such provisions for the seismic design of composite structural steel and reinforced concrete buildings has begun by the Building Seismic Safety Council (BSSC). They are based upon the 1994 National Earthquake Hazards Program (NEHRP) Provisions and subsequent modifications made in the 1997, 2000, and 2003 NEHRP Provisions and in ASCE 7-05 (ASCE, 2005).

The 2005 AISC Seismic Provisions include updated seismic design standards for composite structure systems

Table 1. The summary for composite-moment frame (C-MF) structures

C-MF Type	Yield Shape and Main Deformation	SDC	Moment Connections	Other System Requirements
C-PRMF	Limited yielding occurs in column base and main yielding occurs in the ductile components.	C or below	A nominal strength is at least equal to 50 percent of Mp. Connections shall be capable of sustaining the total inter-story drift of 0.04 rad.	Composite beams shall be encased and fully composite. The stiffness of beams shall be determined by EIeff for the composite section.
C-SMF	Limited inelastic deformations occur in the columns and/or connections and main yielding occurs in the beams.	D and above	The required strength shall be determined with the expected flexural strength (R_yMn). Connections shall be capable of sustaining the total inter-story drift of 0.04 rad.	Composite columns shall meet the requirement of the special seismic systems of Sec. 6.4 or Sec. 6.5 (ANSI. 360-05), as appropriate.
C-IMF	Moderate inelastic deformations occurs in the columns and/or connections and main yielding occurs in the beams	C and below	The required strength of connections shall be based on the plastic capacity of steel beams. Connections can sustain the total inter-story drift of 0.03 rad.	Composite columns shall meet the requirement of the intermediate seismic systems of Sec. 6.4 or Sec. 6.5 (ANSI. 360-05), as appropriate.
C-OMF	The limited inelastic action will occur in the beam, columns and/or connections	A and B	Connections can sustain the total inter-story drift of 0.02 rad.	Composite columns shall meet the requirement of the ordinary seismic systems of Sec. 6.4 or Sec. 6.5.

such as composite connections, composite moment frames, composite braced frames, and shear walls. They incorporate both the Allowable Stress Design (ASD) and Load and Resistance Factor Design (LRFD) methods. As mentioned above, four potential classes of Composite Moment Frame (C-MF) can be identified in these provisions shown. The summarized characteristics for C-MFs are shown in Table 1. The primary purpose of these provisions is to provide information useful to determine the required strength, inter story drift, and seismic use group. Seismic Design Category (SDC) assigned to a building is the classification based upon the occupancy class and the seismicity of the site. SDC A, B and C are generally applicable to structures with the moderate seismic risk, while SDC D, E, and F are necessary to special seismic provisions which cover the areas of high seismic risk.

The performance of composite special moment frame (C-SMF) structures in high seismic area will be treated in this research with entire satisfaction of the new design code requirements. C-SMFs are composed of a variety of configurations where structural steel or composite beams are combined with either reinforced concrete or composite columns. Steel beam-to-CFT column connections with I-girders have been widely used in C-SMF systems for building in Japan, as shown in Fig. 1, and there have been recent researches resulting in practical design recommendations (Azizinamini and Schneider, 2001). Based on ASCE 7-05 (ASCE, 2005), C-SMFs were originally designed for use in SDC D and above. C-SMF shall be designed with assumption that significant inelastic deformation will occur under the design earthquake, primarily in the beams, but with limited inelastic deformation in the columns and connections. Therefore, connections in the C-SMF satisfy the story drift capacity of 0.04 radians as specified in the AISC 2005 Seismic Provisions so that they are not susceptible to fracture at the welded area.

3. Design of Prototype Frames

The SAC represents a joint project that has studied steel connections and structural systems in the aftermath of 1994 Northridge and 1995 Kobe earthquakes. The SAC model structures designed as a part of this joint project are commonly applied to reference examples when evaluating the performance of new or updated structural systems. Three sets of ordinary office buildings were designed with 3-, 9-, and 20-story SAC post-Northridge composite-moment resisting frames assumed to be located in a stiff soil area of downtown Los Angeles (FEMA, 2000). The plan and elevation views of SAC model buildings are illustrated in Fig. 2. The members selected for the girders are also shown in this figure. The perimeter moment frames designed to resist lateral movement are marked by bold lines along the beam members. The CFT column bases were considered to be clamped at the base in the 3-story building. On the other hand, the column bases in the 9- and 20-story building were modeled as pinned-end supports and basement levels were restrained against lateral displacement.

This soil condition for LA buildings was defined as soil type D in the ASCE 7-05. Each set of buildings was constructed with either rectangular CFT (RCFT) columns or circular CFT (CCFT) columns. The buildings in LA area, for the 2% probability of exceedence in 50 years, were designed with the mapped spectrum accelerations corresponding to LA 90045 area as defined by S_S=1.60 g

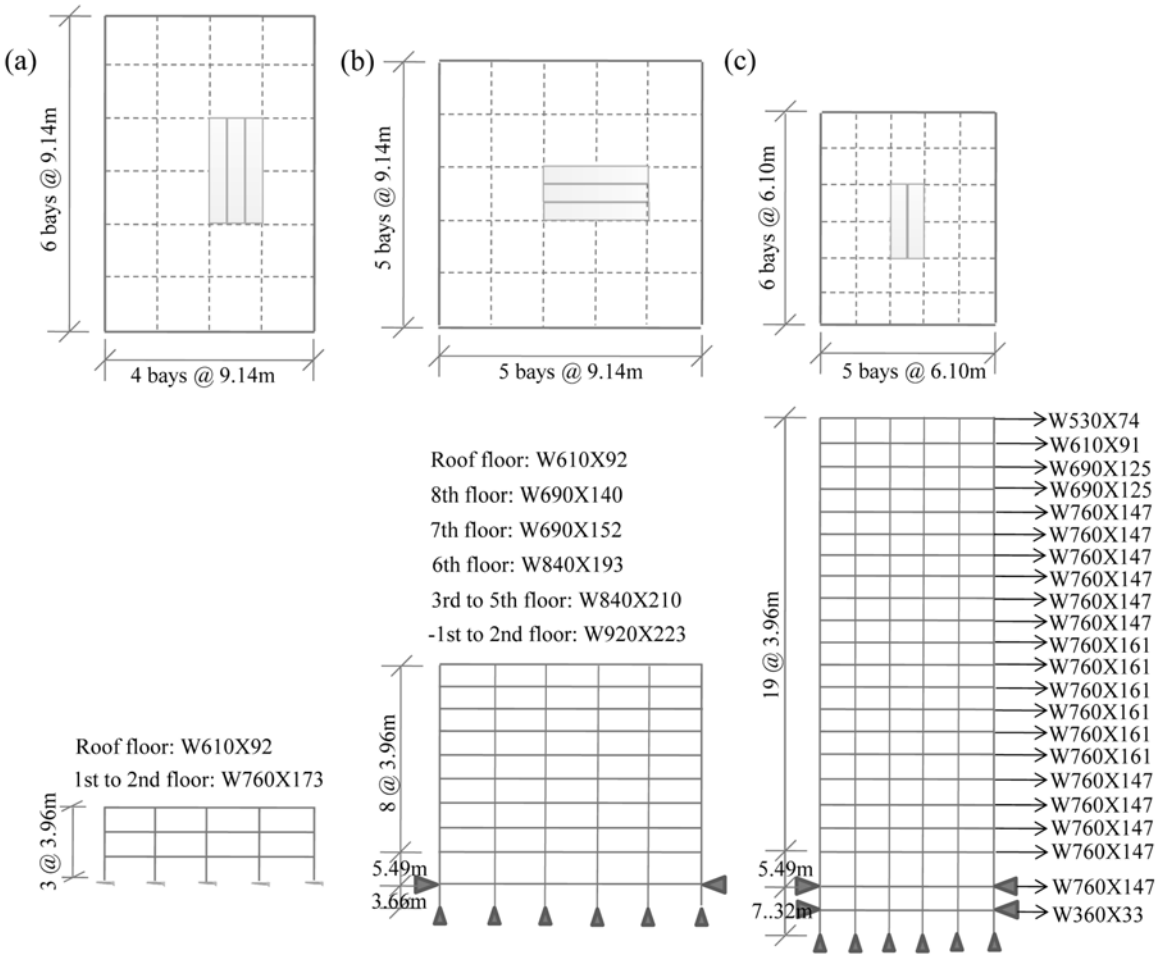

Figure 2. Floor plans and elevations for composite-moment frames: (a) 3 story bay; (b) 9 story bay; (c) 20 story bay.

for the short period and S_1=0.60 for 1 second period. The mass including gravity loads plus partial live loads (approximately 20%) conformed to code requirements for seismic design as specified in Appendix B of the FEMA 355C (FEMA, 2000). The importance factor (I_E) of 1.0 was assigned to the buildings in accordance with Occupancy Category I or II because of ordinary structures. The response modification factor (R) and the deflection amplification factor (C_d) for special composite steel and concrete moment frames was taken as 8 and 5.5, respectively, as specified in Table 12.2-1 of the ASCE 7-05 (ASCE, 2005). Other basic conditions applied to the building design are summarized in Table 2.

Elastic analyses performed by the OpenSEES and SAP2000 program (CSI, 2007) were used to estimate inter-story drifts, deflections, and P-Delta effects. After this initial analysis, a design check was run by using an AISC-LRFD 2001 code (AISC, 2001) which is available on the design check menu of the SAP2000 program. Only dead (DL), live (LL), and earthquake (E) loads are considered in the design check as earthquakes dominate over wind loads in the western US area. Moreover, the earthquake effect includes the component from both vertical and horizontal accelerations. In substitute for earthquake loads, the equivalent lateral loads (E) for the elastic analyses of these composite frames were computed by using the IBC 2006 and ASCE 7-05. The dominant load factors and combination for elastic analyses as specified in these design guideline result in load combination 5 (LC5=1.2DL+1.0E+1.0LL) (ASCE, 2005).

The ASCE 7-05 requires that the inter-story drift (Δ) should not exceed the allowable inter-story drift (Δ_a) as obtained from Table 12.12-1 of the ASCE 7-05 for any story levels. The inter-story drift can be calculated as the difference of the elastic deflections (δ_i) at the top and bottom of each story level as shown in Fig. 3. The elastic deflections of each story level x and allowable inter-story drifts are determined as following equations:

Table 2. The Basic conditions applied to the building design

Located Area	Gravity Loads	SDC	Site Condition	Occupancy Category
LA Area	Dead: 4.12 kPa Live: 2.39 kPa	D Class	Stiff Soil (Site Class D)	Ordinary Structures

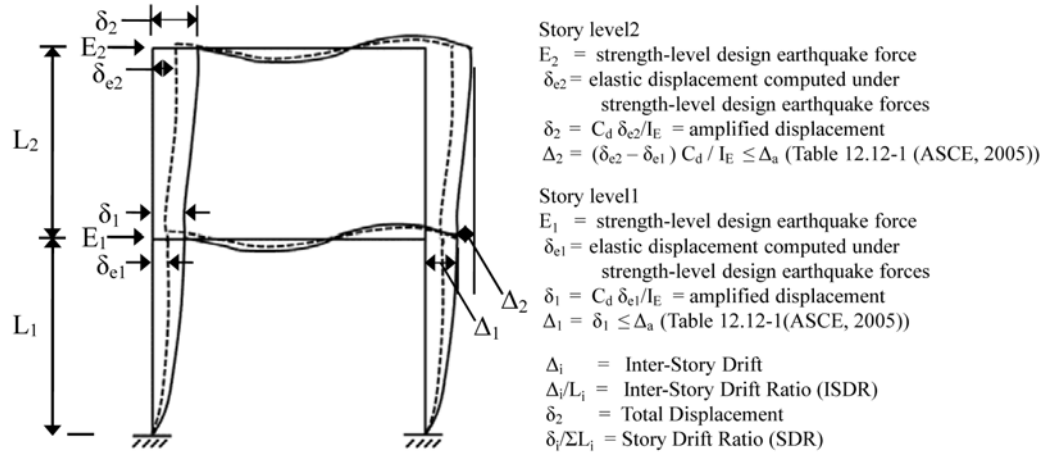

Figure 3. Story drift determination (ASCE, 2005).

$$\delta_i = \frac{C_d \delta_{ie}}{I_E} \quad (1)$$

$$\Delta_a = 0.02 h_{ie} \quad (2)$$

where,

δ_{ie}: deflections determined by an elastic analysis for C-SMF system

h_{ie}: story height at each story level i.

The inter-story drift additionally caused by the P-Delta effect need not be considered when the stability coefficient (θ) is less than or equal to 0.1. The stability coefficient is determined by:

$$\theta = \frac{P_i \Delta}{V_i h_{si} C_d} \quad (3)$$

where,

P_i: total un-factored vertical design load at and above story level i

V_i: seismic lateral force between story level i and story level i-1

h_{si}: story height below the level i.

The stability coefficient shall not exceed θ_{max} determined as below:

$$\theta_{max} = \frac{0.5}{\beta C_d} \leq 0.25 \quad (4)$$

where, β is the ratio of shear demand to shear capacity for the story between story level i and story level i-1, generally taken as 1.0.

Based on these limits, the design checks for deflection and drift limits for the composite frames can be conducted by comparing the factored deflections obtained by Eq. (1) and the stability coefficient by Eq. (3) with the allowable story drift and the stability coefficient limit (0.1 or θ_{max}), respectively. The design checks of deflection and drift limit for the C-SMF subjected to the dominant LC 5 will be shown after the initial selection of member sizes using the OpenSEES program. The initial selection of CFT column members is given to Table 3. The first number and letter of the acronym shown in the model ID indicates the total numbers of stories (i.e., 3S or 9S). The remainder of the letter indicates the CFT column type used (i.e., RCFT: Rectangular CFT, CCFT: Circular CFT). Each set of prototype frames was constructed with RCFT or CCFT columns. A uniform size for all column members over the story height was selected on either exterior or interior columns because of fabrication and economy considerations.

4. Analytical Models

In this section, the modeling attributes for the 2D numerical frame models which will be used for nonlinear analyses are described. This includes, in particular, panel zone modeling following mostly OpenSEES. The general modeling methods for the numerical frame models are also introduced in the guidelines given in FEMA 355C (FEMA, 2000).

The composite columns and steel beams were modeled as nonlinear beam-column elements. 2D discrete fiber sections placed in the integration points of nonlinear beam-column elements can simulate the cross section of

Table 3. The size of CFT columns (SI unit)

Model ID	RCFT Column		Model ID	CCFT Column	
	Exterior Column	Interior Column		Exterior Column	Interior Column
3SRCFT	HSS254X254X10	HSS254X254X10	3SCCFT	HSS286X12	HSS286X12
9SRCFT	HSS406X406X12	HSS406X406X16	9SCCFT	HSS457X457X12	HSS508X508X12
20SRCFT	HSS356X356X16	HSS406X406X16	20SCCFT	HSS457X457X12	HSS508X508X12

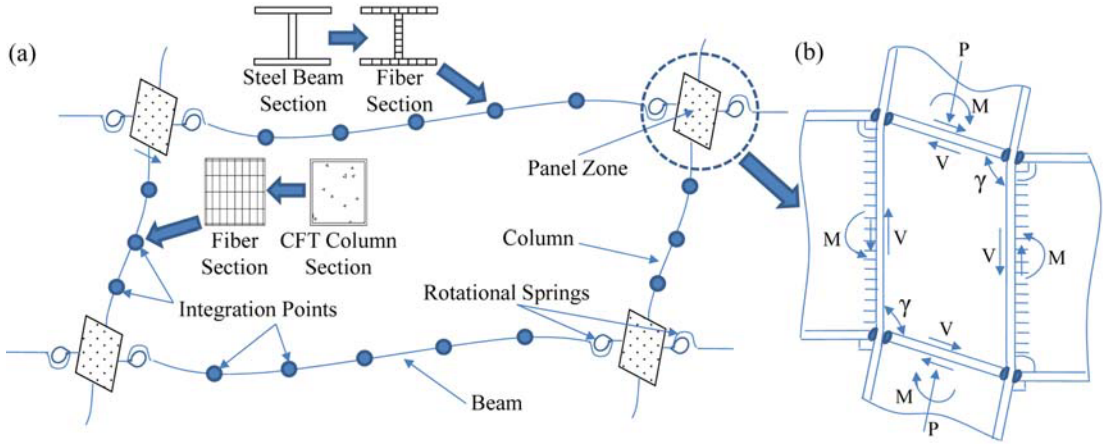

Figure 4. Numerical modeling attributes for composite-moment frames (C-MFs) included panel zone model with rigid boundary elements and nonlinear beam-column elements with 2D fiber sections: (a) Deformed C-MF under seismic loading; (b) Deformed panel zone subjected to seismic loading.

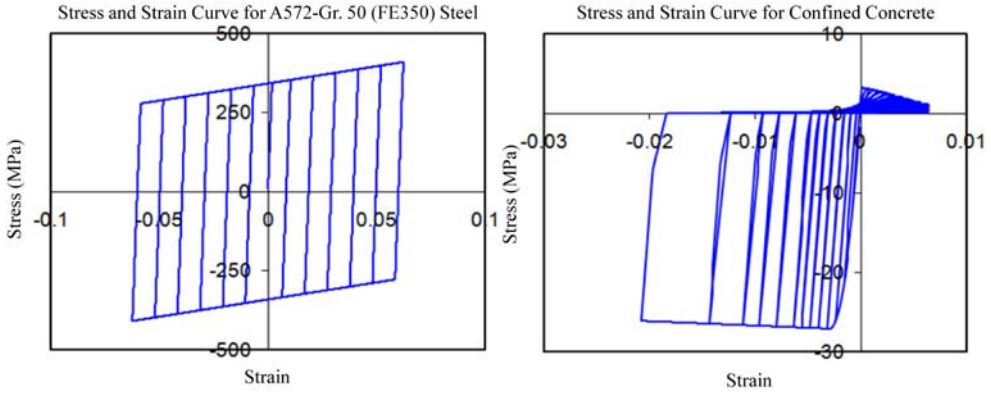

Figure 5. Material properties for the analyses.

CFT columns and steel beams as shown in Fig. 4. The expected material strengths were used in accordance with the material properties shown in Fig. 5. Especially, the material property for concrete contained both different stress-strain curves for tension-compression response and confined effect caused by outside steel tube. The gentle strength degradation after peak strength shown in the material behavior of concrete was due to this confined effect (Hu *et al.*, 2005). All material behaviors applied were simulated using default nonlinear material models provided in the OpenSEES program (Mazzoni *et al.*, 2006). These nonlinear material behaviors were assigned into the nonlinear elements with the 2D discrete fiber sections. All nonlinear analyses were carried out under the same conditions with the following assumptions:

- A mass corresponding to 1.0DL (Dead Load)+0.2 LL (Live Load) was applied for the nonlinear dynamic analyses
- Steel material properties included a 1.5% strain hardening (See Fig. 5)
- A 2.5 % Rayleigh damping was used in the first mode
- Soil-structure interaction at the ground support was neglected
- The beams and columns extended from centerline to centerline
- The uniform loads on the beams were converted into equivalent point loads
- A beam was modeled as many nonlinear beam-column elements subjected to the equivalent point loads
- Dimensions, strength, and stiffness of panel zones are considered in order to evaluate the structural performance more accurately in the performance-based design.

The most significant characteristic of frame analyses presented in this study is the careful consideration of the panel zone modeling. The behavior of connections can be simulated reasonably well by using the more precise 2D joint elements originally developed by Altoontash (Altoontash, 2004) as shown in Fig. 6. These joint elements were installed on the panel zones of numerical frame models as shown in Fig. 4 (a). Fig. 4 (b) shows the idealized force distribution at the perimeter of the joint for a deformed connection subjected to seismic loads. Generally, the beam develops its flexural strength (i.e., plastic hinging) while the column carries the axial gravity loads (P) elastically. In addition, the composite panel

zone at the beam-to-column connection deforms by the internal shear forces (V). Thus, the 2D joint element consisted of rotational springs, internal nodes, and rigid elements in an effort to simulate the exact behavior of connections under these response mechanisms. 4 External nodes determined the size of panel zones. They also connected beam or CFT column members to each panel zone. The shear panel spring on the internal node should be included to generate a tri-linear behavior of the composite panel zone proposed by Nishiyama *et al.* (2004). Rigid elements on the perimeter were applied in the 2D joint element to simulate shear distortions in the panel zone. The CFT columns were connected to the panel zone without rotational springs at external nodes (i.e., fixed member-end rotation) so that the columns carried the gravity axial loads elastically. On the other hand, the rotational springs were placed on the external nodes of the beam ends to simulate the nonlinear moment-rotational behavior of connection models.

Moment resisting frame systems with moment connections were commonly designed on the basis of the full plastic moment strength of the steel beam, meaning that the plastic hinge occurred at the girder. The rotational angle limit for the connection design provided ductile behavior over a certain range of the total rotational angle demand. For example, in the aftermath of Northridge earthquake, an elastic rotation of 0.01 radians and a plastic rotation of 0.03 radians under cyclic loads, corresponding to the total rotation of 0.04 radians, have been accepted as the rotational limit to distinguish between ductile and brittle connections in special moment resisting frames. The steel beam-to-CFT column connection with cross section continuous through steel tube was incorporated into the analyses of the post-Northridge building study. Fig. 7 shows the cyclic behavior of this connection type obtained from the experimental test performed by Schneider and Alostaz (1998). The ductile connection behavior was characterized by no flexural strength degradation up to a total inter-story rotational angle of 0.04 radians. This figure shows that the ultimate flexural strength deteriorates slowly as the local buckling of the beam flange occurs. The connections was able to develop the ultimate moment at the CFT column face approximately 1.25 times the full plastic moment strength of the beam. Therefore, the connection design meets the requirement of the C-SMF structure. Comparisons of the simulated moment-rotation angle curves and the experimental response for full connection tests (Schneider and Alostaz, 1998) are also shown in Fig. 7. These curves should be calibrated based on the experimental test result. The more precise calibration including strength degradation can be found at the curve simulated by the 2D joint element than that by the conventionally used rigid joint model. Only 2D joint model was used for nonlinear 2D frame analyses to capture the significant attributes of experimental test results such as strength degradation and Bauschinger effect.

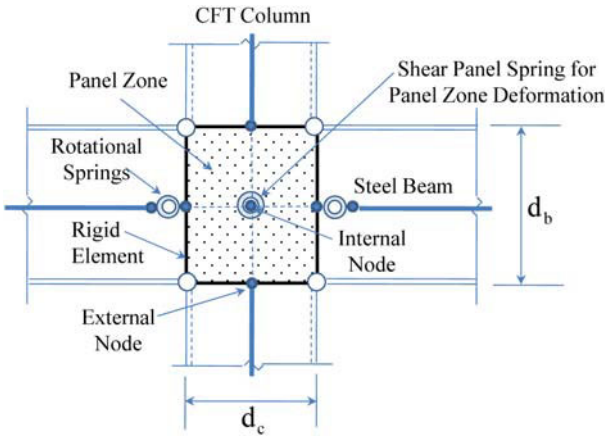

Figure 6. 2D joint element with rigid boundary elements (Altoontash, 2004).

5. Analytical Study

5.1. Seismic design loads

The static pushover and dynamic analyses were performed on each numerical frame model using the OpenSEES program to evaluate its lateral resistance strength and post-yield behavior. Moreover, these seismic performance on the frame structures were first estimated through static pushover analyses. The distributions of equivalent lateral loads (E) for the pushover analyses were determined by a set of static lateral loads that corresponded to the 1st mode shape of deformation as introduced in the ASCE 7-05 and the IBC 2003 codes. For frame structures, the first mode generally contributes upwards of about 90% of the effective seismic mass and dominates the behavior of the structure. However, this procedure may not always be valid when higher mode shapes contribute more than 10% of the effective seismic mass (Padgett and DesRoches, 2008). The mass values were applied to numerical frame models so as to calculate the elastic modal properties of the structure including modal periods, modal participation factors, and modal mass ratios for the first three modes. These elastic modal properties for three frame models are summarized in Table 4. The first mode results in the dominant mode shape because it occupies most of modal mass ratios. Therefore, as specified in the design guidelines, the formation of equivalent lateral loads depends on the elastic modal property of the structure in the first mode.

The design response spectrum for area code 90045 (LA) is shown in Fig. 8. This design spectrum curve shall be developed using the mapped spectrum acceleration parameters and site condition as indicated in Sec. 11.4.5 of the ASCE 7-05. The fundamental time period of the selected frame models marked on the figure (e.g., T=1.52 sec for 9SRCFT and T=2.74 sec for 20SRCFT) were obtained from elastic modal analyses in the first mode. For conservative design, the fundamental time period (T) shall not exceed the product of the upper limit coefficient on calculated period (C_u) from Table 12.8-1 of the ASCE

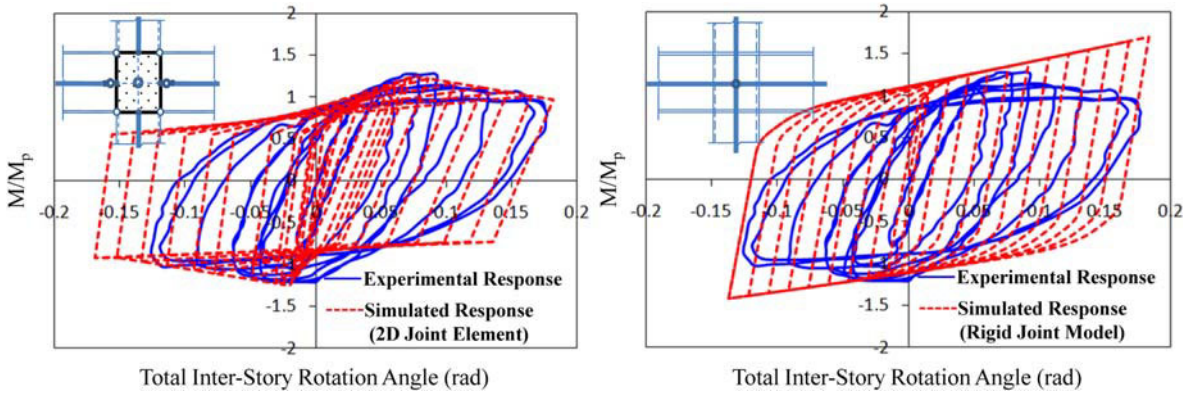

Figure 7. Comparisons of the simulated moment-rotation angle curves and the experimental response for Schneider and Alostaz (1998).

Table 4. Elastic modal properties of C-MF structures

Model ID	Elastic Modal Property	Mode 1	Mode 2	Mode 3	Model ID	Elastic Modal Property	Mode 1	Mode 2	Mode 3
3SRCFT	Time Period*	0.975	0.319	0.175	3SCCFT	Modal Period	0.962	0.313	0.171
	Modal PF**	1.126	-0.402	0.155		Modal PF	1.102	-0.387	0.147
	Mass PF**	0.875	0.109	0.016		Mass PF	0.873	0.111	0.016
9SRCFT	Modal Period	1.517	0.537	0.307	9SCCFT	Modal Period	1.485	0.526	0.300
	Modal PF	2.132	-0.724	0.354		Modal PF	2.129	-0.729	0.359
	Mass PF	0.875	0.100	0.024		Mass PF	0.874	0.102	0.025
20SRCFT	Modal Period	2.742	0.925	0.539	20SCCFT	Modal Period	2.456	0.908	0.528
	Modal PF	2.373	-0.841	0.425		Modal PF	2.365	-0.849	0.434
	Mass PF	0.866	0.107	0.028		Mass PF	0.864	0.109	0.028

* Unit is Second. ** PF: Participation Factor

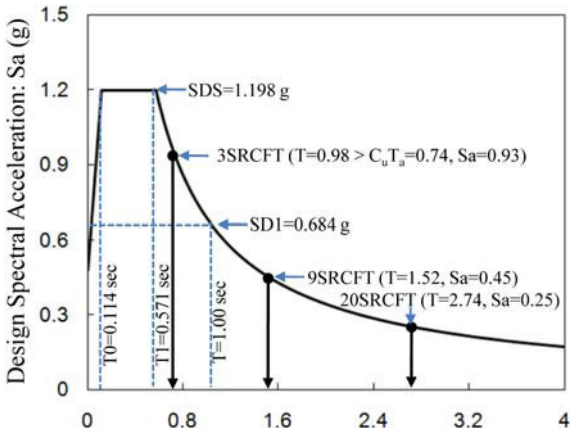

Figure 8. Design response spectra for C-MF in LA area.

7-05 and the approximate fundamental time period (T_a) obtained from Sec. 12.8.2.1 of the ASCE 7-05. As a result, the upper limit of the fundamental time period (C_uT_a=0.74 sec) should be used for the design of 3SRCFT model on the ground that the fundamental time period determined from the analysis (T=0.98 sec) exceeds this upper limit.

After computing the design spectral acceleration (Sa), the seismic response coefficient (Cs) should be determined in accordance with Sec. 12.8.1.1 of the ASCE 7-05 in order to develop the seismic design base shear force (Vs). This base shear force was calculated from the product of seismic response coefficient and total effective seismic weight, so that Vs=CsW. To generate the equivalent lateral seismic forces (E) induced at any story level, the seismic design base shear force should be distributed into the various vertical members of the seismic force resisting system under consideration based on both the portion of structural seismic weight at each story and the fundamental time period of the moment frame structure in the first mode. According to each selected frame model, the vertical distribution factors for the seismic design base shear forces over each story level (CV_i) are shown in Fig. 9. This vertical distribution factors correspond to the first mode shape of deformation. The first three elastic mode shapes are also shown in Fig. 9.

5.2. Nonlinear static pushover analyses

The dominant load combination including a set of equivalent lateral loads (i.e., LC5) was applied to the frame models for nonlinear static pushover analyses. Force and displacement relationships obtained from these pushover analyses were occasionally used to estimate the

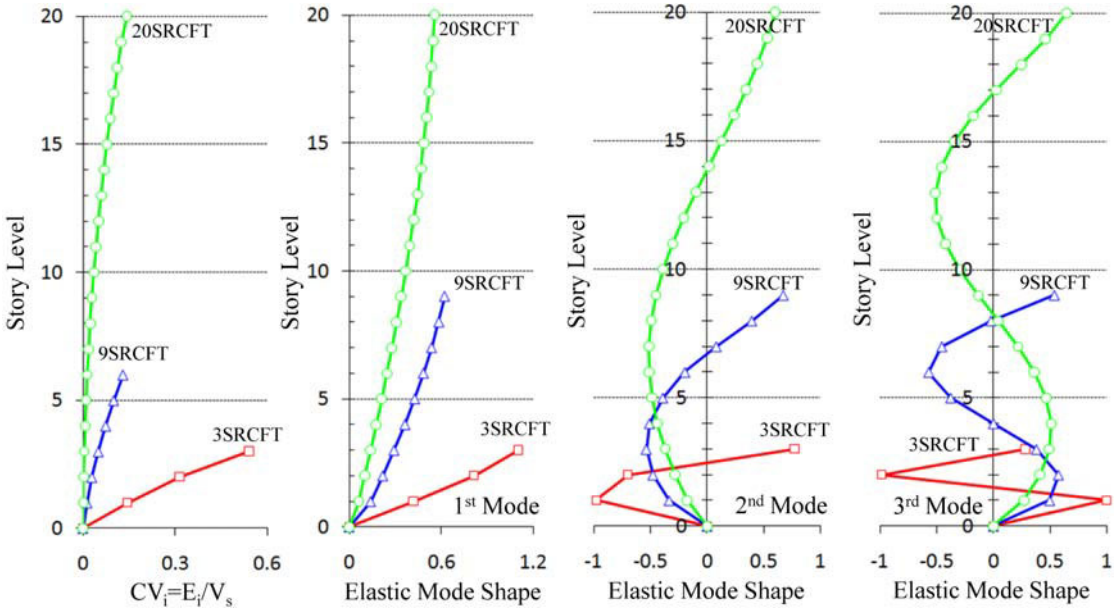

Figure 9. Elastic mode shapes of the first three modes.

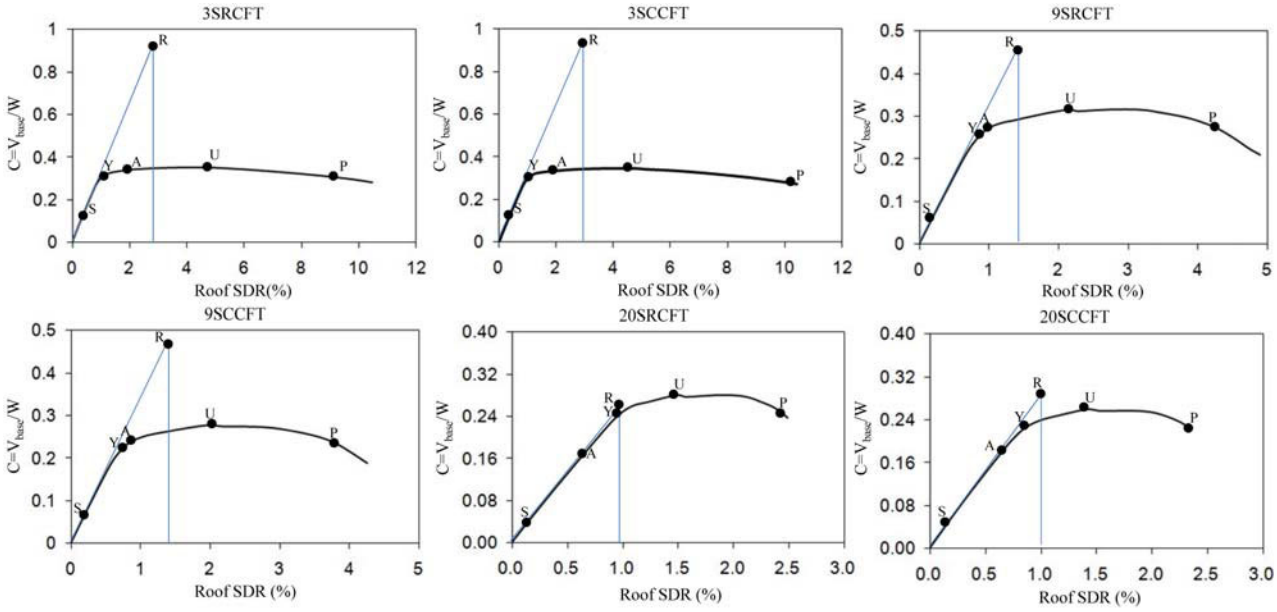

Figure 10. Pushover curves for C-MF structures.

capacity of the frame structure undergoing considerable inelastic deformation. These relationships can be converted to the seismic base shear coefficient (C) and roof story drift ratio (SDR). The seismic base shear coefficient was calculated from the ratio of the base shear force to the total effective seismic weight ($C=V_{base}/W$). The roof story ratio was calculated from the roof displacement normalized by the total story height. For the frame models under a set of equivalent lateral loads, the normalized pushover curve can be approximated by a bi-linear curve that represents two base shear levels: (1) a yielding base shear (Point Y) and (2) an ultimate base shear (Point U). Besides two base shear levels, the base shear points at the seismic design base shear (Point S), response modification factor (Point R), deflection amplification factor (Point A), and stability limit (Point P) were added to the pushover curves.

Figure 10 shows the resulting pushover curves plotted as the seismic shear coefficient-roof SDR relations for the 3-, 9-, and 20-story frame structures. According to the different base shear levels for each frame model, the relevant result such as corresponding roof SDR and over-strength ratio is also given to Table 5. The over-strength ratio was defined herein as the ratio of the base shear force at each observation point to the seismic design base shear force ($\Omega=V/V_s$). This over-strength ratio may be observed by using displacement-control increments in the OpenSEES program and are very useful to investigate the

Table 5. The result of pushover analyses

Model ID	Design Point (S) Ω_S=1.00	Yield Point (Y)	Ductile Point (A)	Elastic Point (R) Ω_R=8.00	Ultimate Point (U)	Stability Point (P) CY=CP	Seismic Weight (W)
3SRCFT	C_S=0.116 Δ_S=0.349%	C_Y=0.296 Δ_Y=0.927% Ω_Y=2.55	C_A=0.333 Δ_A=1.920% Ω_A=2.87	C_R=0.928 Δ_R=2.840%	C_U=0.3460 Δ_U=4.420% Ω_U=2.98	Δ_P=9.182%	W=2130 kN
3SCCFT	C_S=0.116 Δ_S=0.339%	C_Y=0.281 Δ_Y=0.874% Ω_Y=2.42	C_A=0.339 Δ_A=1.865% Ω_A=2.92	C_R=0.928 Δ_R=3.153%	C_U=0.3524 Δ_U=4.257% Ω_U=3.03	Δ_P=10.44%	W=2130 kN
9SRCFT	C_S=0.056 Δ_S=0.175%	C_Y=0.257 Δ_Y=0.883% Ω_Y=4.58	C_A=0.269 Δ_A=0.963% Ω_A=4.80	C_R=0.448 Δ_R=1.425%	C_U=0.3151 Δ_U=2.151% Ω_U=5.62	Δ_P=4.429%	W=7810 kN
9SCCFT	C_S=0.058 Δ_S=0.174%	C_Y=0.231 Δ_Y=0.803% Ω_Y=3.98	C_A=0.245 Δ_A=0.957% Ω_A=4.22	C_R=0.464 Δ_R=1.424%	C_U=0.2764 Δ_U=2.017% Ω_U=4.77	Δ_P=3.840%	W=7810 kN
20SRCFT	C_S=0.031 Δ_S=0.117%	C_Y=0.244 Δ_Y=0.972% Ω_Y=7.87	C_A=0.167 Δ_A=0.644% Ω_A=5.39	C_R=0.248 Δ_R=1.007%	C_U=0.2805 Δ_U=1.502% Ω_U=9.05	Δ_P=2.451%	W=7670 kN
20SCCFT	C_S=0.033 Δ_S=0.114%	C_Y=0.227 Δ_Y=0.870% Ω_Y=6.88	C_A=0.174 Δ_A=0.627% Ω_A=5.27	C_R=0.264 Δ_R=1.006%	C_U=0.2602 Δ_U=1.437% Ω_U=7.88	Δ_P=2.279%	W=7670 kN

strength of a structure for the seismic evaluation.

Moment frames behave as linearly elastic until the first yielding occurs at the CFT column bases. For the 3SRCFT model, the yielding base shear force corresponded to C_Y=0.296 and V_Y=631 kN. This was larger than the seismic design base shear force (C_S=0.116 and Vs=247 kN) because the yielding over-strength ratio exceeded 1.0 (Ω_Y=2.55). Except for 20-story frame models, ductile points (Point A) referred to as the magnified elastic deflections were located on the inelastic range of the pushover curve. The elastic base shear was the product of the seismic design base shear and a response modification factor, so that C_R=0.928 and V_R=1977 kN at an elastic roof SDR of Δ_R=2.840% (Point R). The triangular area shown in each figure represents the total elastic energy or energy demand (E_d). In order to prevent a sudden collapse due to larger P-Delta effect after ultimate strength, the energy capacity (E_c) referred to as the area under the pushover curve should be greater than this energy demand. The average roof SDR level where the negative stiffness was observed for 3-, 9-, and 20-story frames was approximately 9.81%, 4.14%, and 2.37%, respectively. This level coincided with the stability point (Point P). Therefore, the effect of P-Delta increases continuously as the total story height increases. For the seismic design, 20-story frame models required the larger over-strength ratios than other frame models in an effort to guarantee the energy capacity which exceeds the energy demand. After yielding in the CFT column bases, the base shear force entered a hardening range and arrived at the ultimate base shear force (i.e., C_U=0.364 and V_U=776 kN for 3SRCFT). All post-Northridge C-SMF buildings had high ultimate over-strength ratio ranging from 2.98 to 9.05.

Based on the results of nonlinear analyses, a more comprehensive study for C-SMFs was conducted to assess their seismic performance and the extent of structural damage suffered. The performance levels resulting from the transition points on the static pushover curves were used as the story drift limits. The SDRs at the seismic design, yielding, and ultimate base shear point level are shown in Fig. 11. The applied performance levels refer to the difference in the base shear forces (V). For example, V_Y=2010 kN and V_Y=1804 kN were the yielding base shear force of 9SRCFT and that of 9SCCFT, respectively. All frames were stable up to the yield strength level. After reaching the ultimate strength level, plastic deformations began to migrate to the CFT column sections and concentrated on the lower stories. The distributions of SDRs over the story heights were uniform until the yield strength level, but they gradually moved to the lowest level as the lateral loads increased. The increased plastic deformations at the lower story can cause this shift.

5.2. Nonlinear dynamic analyses

The nonlinear dynamic analyses consisted of two suites of earthquake ground motions with 2% probability of exceedence in 50 years for the western USA area (Los Angeles (LA) and Seattle area (SE)). These 40 ground motions (LA21 to LA40 and SE21 to SE40) were developed from both historical records and simulations as part of the FEMA/SAC project on the steel moment frames (Somerville *et al.*, 1997). One ground motion was selected to examine displacement time histories of the roof level. A selected LA21 ground motion and time

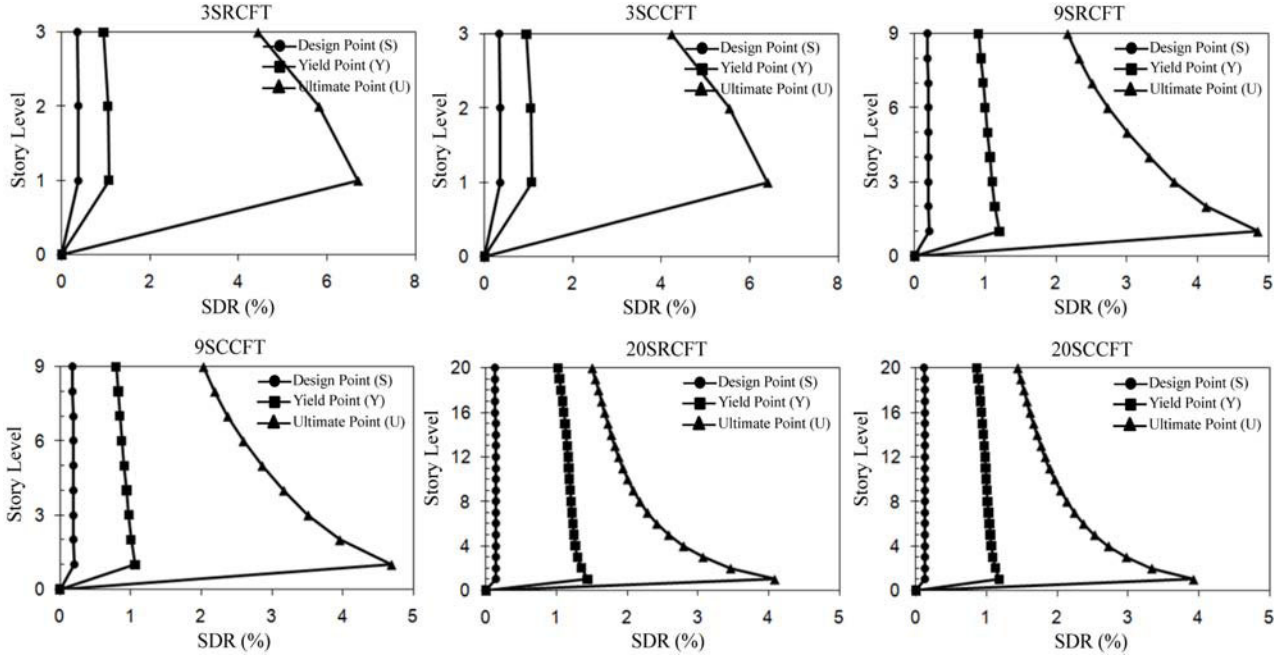

Figure 11. SDRs over the story heights at each roof SDR level (i.e., Design, yield, and ultimate point).

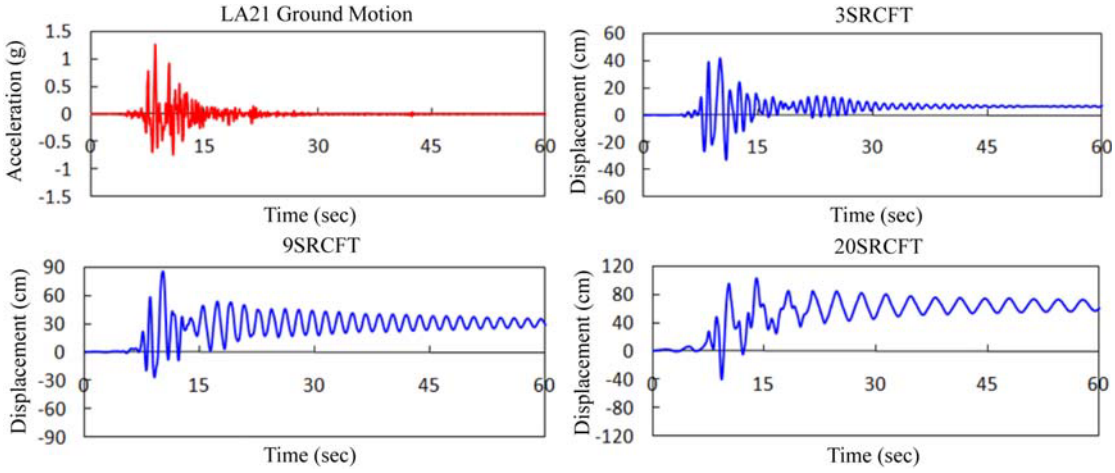

Figure 12. Results of nonlinear dynamic analyses (Displacement time history at the roof).

versus displacement response at the roof story is shown in Fig. 12. This ground motion has a relatively long duration (60 sec.) with a peak ground acceleration (PGA) value of 1.280 g. The PGA for LA 21 ground motion occurred at 8.56 second. The occurrence time for each peak displacement value lagged behind the PGA, so that these peak displacements for 3-, 9-, 20-story frames occurred at 10.0, 10.2, and 14.0 second, respectively. Those for 3-, 9-, 20-story frames were approximately 41.4, 84.9, and 103.0cm, respectively, representing the roof SDR of 3.48, 2.28, and 1.25%. The permanent roof displacement continuously increases as the total story height increases. This larger permanent displacement associated with the total story height can be attributed to larger P-Delta effect and rapid strength degradation as also shown in the pushover curves.

The cyclic behaviors of frame models under LA21 ground motion are also plotted as the seismic base shear coefficients versus roof SDRs as shown in Fig. 13. These plots show the influence of the applied ground motion and the seismic weight. The slightly higher level of ultimate seismic base shear coefficients was observed at the results obtained from nonlinear dynamic analyses in comparison with those from static pushover analyses, representing about 5%.

6. Design Limit and Statistical Investigation

This study has investigated whether the post-Northridge C-SMFs presented herein can meet the design limits specified in Eq. (1) to Eq. (4). The elastic design

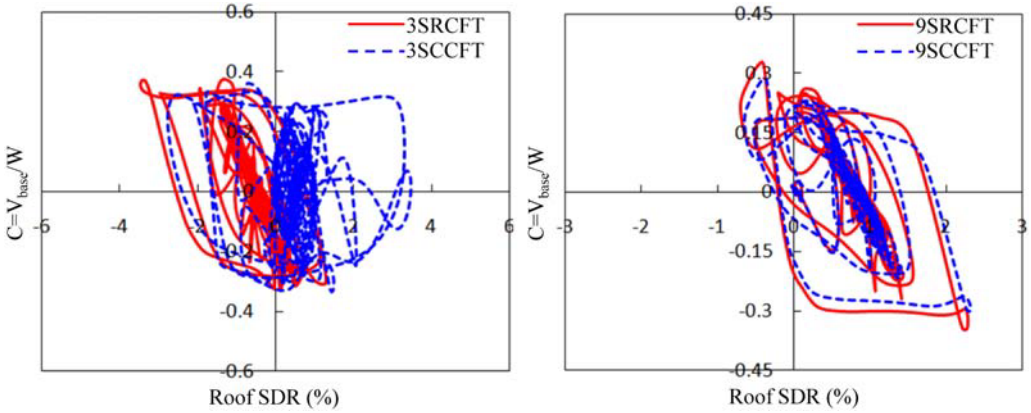

Figure 13. Results of nonlinear dynamic analyses (Normalized base shear force vs. Roof SDR).

deflections between two inter-stories, as determined by Eq. (1), should not exceed the allowable inter-story drift (Δ_a). Fig. 14 shows the inter-story drift ratio (ISDR) which results in the percentile ratio of the inter-story deflection to its story height (i.e., ISDR=$100\delta_i/h_{ei}$). The value of 2% ISDR derived from Eq. (2) became the design limit for the elastic inter-story deflection. The ISDRs of 3-story frames at the lower story level were very proximate to the design limit. Note that their ultimate over-strength ratios obtained from static pushover analyses are also very close to the over-strength ratio specified in Table 12.2-1 of the ASCE 7-05 (Ω=3.0). On the other hand, 9- and 20-story frames where the ultimate over-strength ratios were much more than 3.0 had a wide margin to the allowable design limit value of 2% ISDR. It represents that the relatively large size of CFT columns was used for the design of these frames. All frame designs satisfied this design limit all over the story level as shown in this figure.

The stability coefficient as determined by Eq. (3) can be applied to the design check. This coefficient should be equal or less than the design limit. As shown in Fig. 15, the larger stability coefficients concentrated on the lower story level because of the effect of P-Delta. They also decrease as one moves up the frame. The relatively larger stability coefficients were distributed all over the story level of 20-story frames in comparison with that of other frames. The stability coefficients were below the design stability limit which is the value of 0.091 radians calculated by Eq. (4).

In order to examine the dynamic performance and evaluation effectively, the peak responses were investigated.

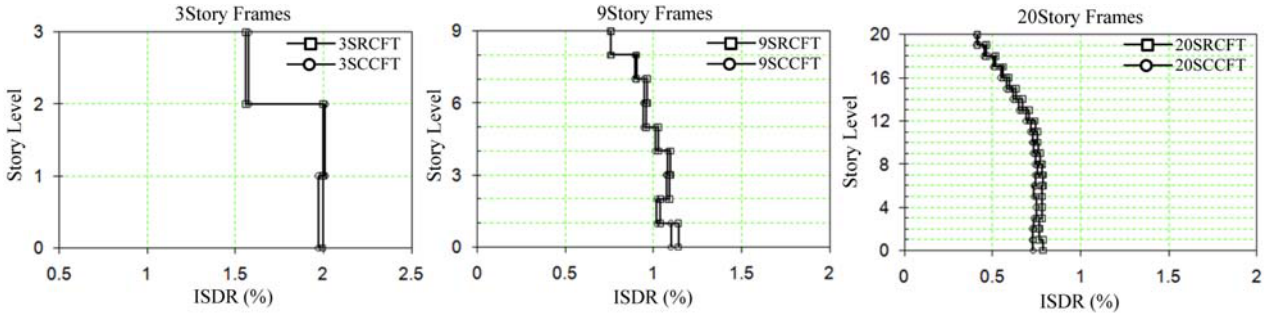

Figure 14. Investigation of the design inter-story drift ratios (ISDRs) within the allowable limit.

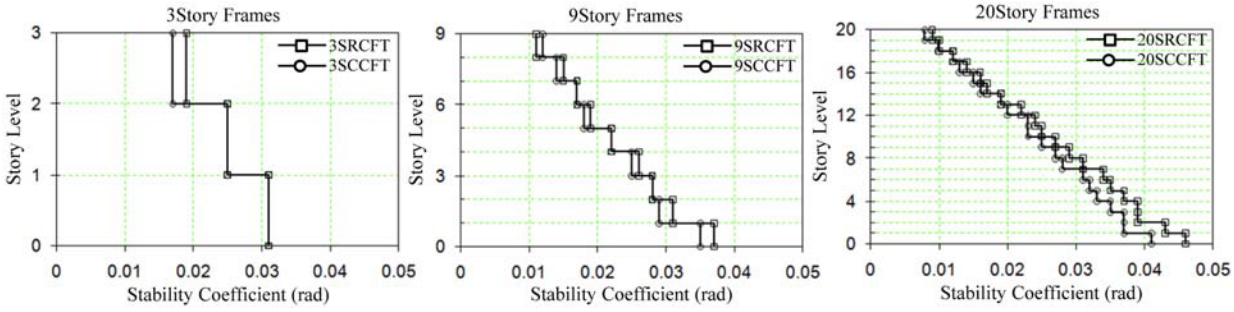

Figure 15. Investigation of the stability coefficients within the allowable limit.

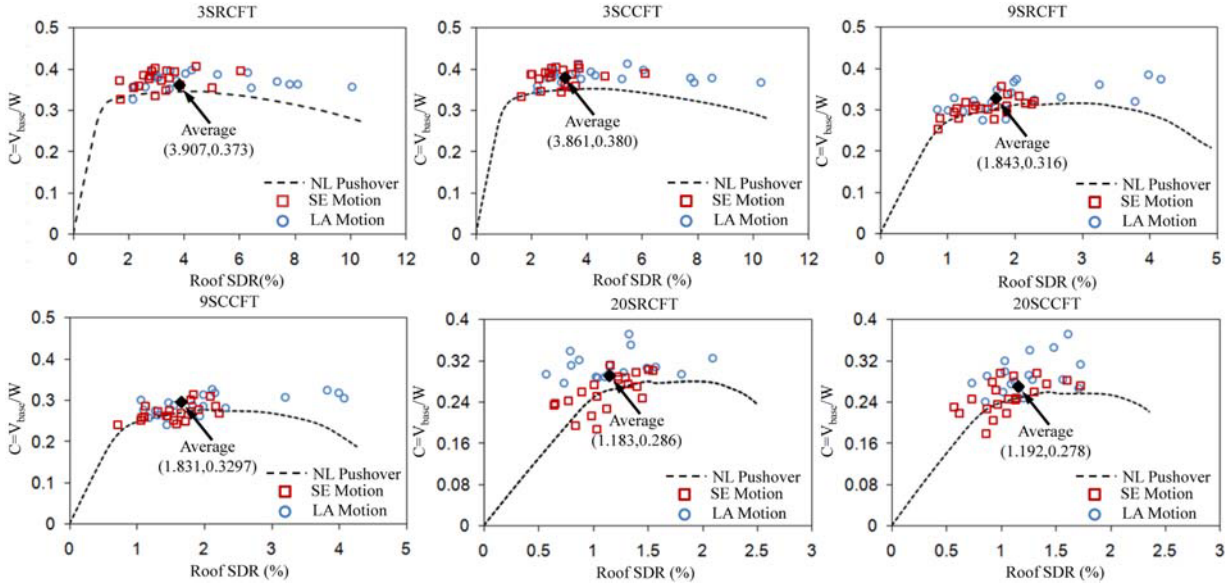

Figure 16. Peak responses at the roof story under 40 original ground motions.

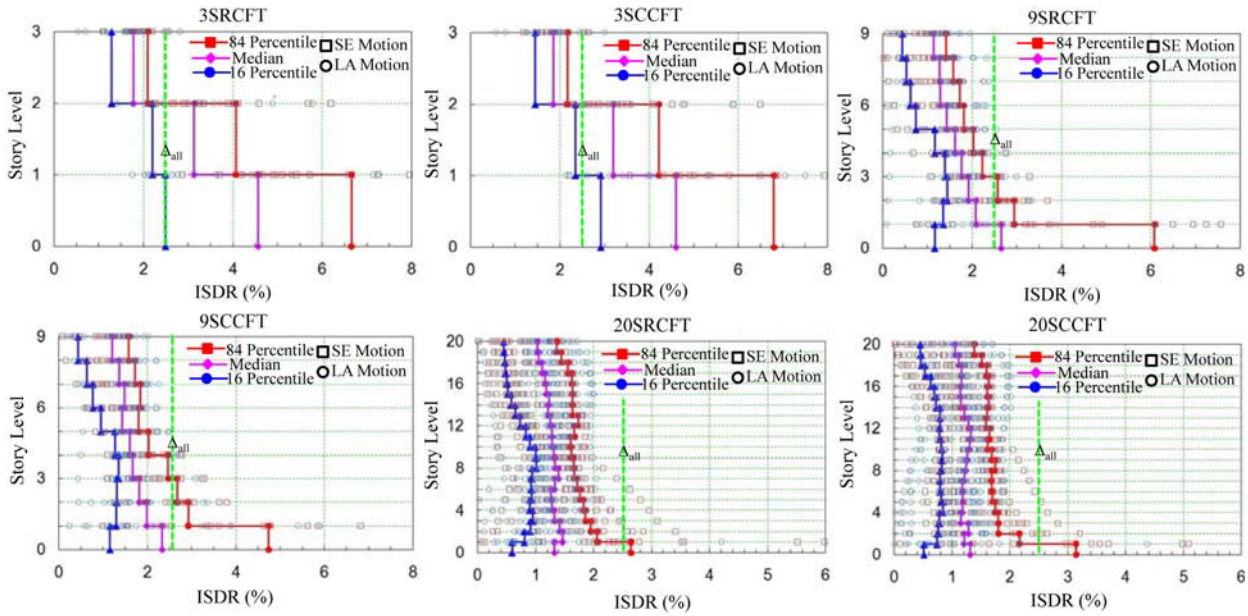

Figure 17. Statistical investigation of the peak ISDRs under 40 original ground motions.

The graphs of the scatter data for peak seismic base shear coefficients versus roof SDRs are provided in Fig. 16, as compared with the previous static pushover curves. The average value of the scatter data was also plotted on each figure. The peak base shear force coefficient obtained by the nonlinear dynamic test was approximately 5 to 10 percent larger than the ultimate base shear force coefficient obtained from the nonlinear pushover test. This numerical discrepancy results from the use of lumped masses. 20-story frame models had the largest maximum base shear force due to the larger mass effect. Generally, the scatter data were mainly in the post-yield range, and were associated with both spread yielding and severe member failure throughout the structures.

For another evaluation, the graphs of scatter data for peak ISDRs are provided in Fig. 17. These graphs show 16 percentile, median, and 84 percentile ISDRs together with individual peak datum points. The values of the 84 percentile employed from here to indicate the statistical values of the peak ISDRs as defined in FEMA 355C (FEMA, 2000). The 16th percentile presented herein results in the statistical values which are the opposite side of the 84th percentile from the median. Similarly to the SDRs at the ultimate point obtained by the nonlinear pushover analysis (see Fig. 11), the peak ISDRs obtained from the dynamic analysis showed the largest values at the first story level. They also decrease as one moves up the frame. This implies that the composite columns

located in the lower story levels are susceptible to severe plastic deformations under these ground motions. In addition to the PGA, the lumped masses have an influence on the peak ISDR. The larger lumped masses can increase the values of the peak ISDR. The allowable inter-story drift ratio based on nonlinear seismic response procedure from Sec. 16.2.4.3 in the ASCE 7-05 (125% of the allowable inter-story drift ratio specified in Sec. 12.12.1 of the ASCE 7-05) was applied to the limit for safety. For 3-story frames, even 16 percentile ISDRs exceed the limit at the lower story level. These frames experienced severe member collapse throughout the whole structure under these types of strong ground motions. It is because the ultimate over-strength ratio with approximately 3.0 results in the underestimation for the demand of peak ISDRs. For 20-story frames, all story levels satisfied the allowable design limit except for the 84 percentile peak ISDR at the first story. In addition, three statistical lines exhibited fairly uniform distribution over the height of the structures. The stable seismic behavior shown in these frames can be attributed to the conservative design with considerable over-strength ratios.

7. Concluding Remarks

The major conclusions from this study are summarized below:

(1) Composite-special moment frames (C-SMFs) ranging from low- to high-rise buildings were designed with CFT columns. They were modeled as 2D numerical frames using both nonlinear pushover and dynamic analyses in order to understand the better seismic performance of such frames and to investigate the adequacy of the design procedure. Moreover, the composite panel zones were modeled as 2D joint elements with a tri-linear backbone curve in an effort to simulate the exact behavior of proposed steel beam-to-CFT column connections.

(2) Static nonlinear pushover analyses utilizing the equivalent lateral load pattern used for design were carried out. Pushover curves plotted as the seismic base shear coefficient versus roof story drift ratio showed significant transition points: elastic range or proportional limit, full yielding of the cross-section, strength hardening, ultimate strength, and strength degradation or stability limit. These limits were affected by means of member slenderness ratios and level of the gravity loads.

(3) The nonlinear dynamic analyses consisted of two suites of 40 earthquake ground motions with 2% probability of exceedence in 50 years for the western USA. The base shear forces were affected by lumped masses converted from the gravity loads, so the 9-story frames showed higher maximum base shears than the 3-story frames. Due to the use of the lumped mass including dead loads plus partial live loads, the peak base shear forces obtained from nonlinear dynamic analyses were slightly larger than the ultimate base shear forces from pushover tests.

(4) Statistical distributions of the peak ISDRs were obtained from the nonlinear dynamic analyses. The peak ISDRs showed the largest values at the first story level. They decrease as one moves up the structure. Finally, frame models which were designed with the over-strength ratio specified in the ASCE 7-05 underestimated the inelastic inter-story deflection caused by strong ground motions in the western US area.

In general, all proposed frame models satisfy the allowable design limits specified in the current design guidelines.

Acknowledgments

This research was supported by WCU (World Class University) program through NRF (National Research Foundation) of Korea funded by the Ministry of Education, Science and Technology (Grant No. R32-2008-000-20042-0). The first author would like to also thank NSF (National Science Foundation) for one year of financial support (Grant No. 0324542) as a post-doctorate fellowship at Georgia Tech.

References

Altoontash, A. (2004). *Simulations and damage models for performance assessment of reinforced concrete beam-column joints*. Ph.D. Dissertation. Stanford University, CA.

AISC (2001). *Manual of Steel construction, Load and Resistance Factor Design (LRFD). 3rd edition*, American Institute of Steel Construction, Chicago, IL.

AISC (2005). *Seismic Provisions for Structural Steel Buildings (ANSI/AISC 341-05)*. American Institute of Steel Construction, Chicago, IL.

AISC (2005). *Specification for Structural Steel Buildings (ANSI/AISC No. 360-05)*. American Institute of Steel Construction, Chicago, IL.

ASCE (2005). *Minimum Design Loads for Buildings and Other Structures (ASCE/SEI No. 7-05)*. American Society of Civil Engineers, Reston, VA.

Azizinamini, A. and Schneider, S. P. (2001). "Moment connections to circular concrete-filled steel tube columns." *Journal of Structural Engineering*, ASCE, 130(2), pp. 213-222.

FEMA (2000). *State of the art report on systems performance of steel moment frames subjected to earthquake ground shaking*. Rep. No. FEMA-355C, Federal Emergency Management Agency, Washington, DC.

Hajjar, J. F. (2002). "Composite steel and concrete structural systems for seismic engineering." *Journal of Constructional Steel Research*, 58, pp. 703-723.

Hu, T., Huang, C. S., and Chen, Z. L. (2005). "Finite

element analysis of CFT columns subjected to an axial compressive force and bending moment in combination." *Journal of Constructional Steel Research*, 62, pp. 1692-1712.

ICC (2006*). International building code 2006 (IBC2006).* International Code Council, Falls Church, VA.

Kim, Y. J., Shin, K. J., and Kim, W. J. (2008). "Effect of stiffener details on behavior of CFT column-to-beam connections." *International Journal of Steel Structures*, 8(2), pp. 119-133.

Lee, K. and Foutch, D. A. (2002). "Performance evaluation of new steel frame buildings for seismic loads." *Earthquake Engineering and Structural Dynamics*, 31, pp. 653-670.

Mazzoni, S., Mckenna, F., and Fenves, G. L. (2006). *OpenSEES command language manual*. Department of Civil Environmental Engineering, University of California, Berkley, CA.

Morino, S., Uchikoshi, M., and Yamaguchi, I. (2001). "Concrete-filled steel tube column system-its advantages." *International Journal of Steel Structures*, 1(1), pp. 33-44.

Nishiyama, I., Fujimoto, T., Fukumoto, T., and Yoshioka, K. (2004). "Inelastic force-deformation response of joint shear panels in beam-column moment connections to concrete-filled tubes." *Journal of Structural Engineering*, ASCE, 130(2), pp. 244-252.

Padgett, J. E. and DesRoches, R. (2008). "Methodology for the development of analytical fragility curves for retrofitted bridges." *Earthquake Engineering and Structural Dynamics*, 37, pp. 1157-1174.

Roeder, C. W. (2000). "Seismic behavior of steel braced frame connections to composite columns." *Connections in Steel Structure*, 4, pp. 51-62.

CSI (2007). *SAP 2000 ver. 11 Steel Design Manual, Computer and Structures*. Computer & Structure, Inc. Berkeley, CA.

Schneider, S. P. and Alostaz, Y. M. (1998). "Experimental behavior of connections to concrete-filled steel tubes." *Journal of Constructional Steel Research,* 45(2), pp. 321-352.

Somerville, P. G., Smith N., Punyamurthula S., and Sun, J. (1997). *Development of ground motion time histories for phase 2 of the FEMA/SAC steel project*. SAC background document, Report No. SAC/BD 97/04.

Tsai, K. C. , Hsiao, P. C., Wang, K. J., Weng, Y. T., Lin, M. L., Lin, K. C., Chen, C. H., Lai, J. W., and Lin, S. L. (2008). "Pseudo-dynamic tests of a full-scale CFT/BRB frame-Part I: Specimen design, experiment and analysis." *Earthquake Engineering and Structural Dynamics*, 37, pp. 1081-1098.

Tsai, K. C., Weng, Y. T., Lin, M. L., Chen, C. H., Lai, J. W., and Hsiao, P. C. (2004). "Pseudo dynamic tests of a full-scale CFT/BRB composite frame." *Proc. the 2004 Structure Congress*, ASCE.